JOURNAL OF MATERIALS SCIENCE 24 (1989) 2011–2017

# Graphite–epoxy laminates with almost null coefficient of thermal expansion under a wide range of temperature

TAKASHI ISHIKAWA, HISAO FUKUNAGA, KOH-ICHI ONO
*Airframe Division, National Aerospace Laboratory, 1880 Jindaiji-Machi, Chofu-shi, Tokyo 182, Japan*

A lamination tailoring technique is proposed in order to control a coefficient of thermal expansion of graphite–epoxy composites in a principal direction. This technique consists of two concepts of the thermoelastic invariants and the lamination parameters. The expansion free condition yields to a parabola in the feasible region of the lamination parameters. The calculated curves for a wide range of temperatures intersect almost at a point. A laminate with the lay-up construction corresponding to this point will exhibit an approximately null coefficient of thermal expansion in one direction in that temperature range. Some preliminary experimental results indicate that the present procedure is possible and promising. The tailored material will be appropriate for the space station structure.

## 1. Introduction

Two of the most attractive points in favour of graphite–epoxy composites are their high specific strength and specific models for their applications in aerospace structures. Another advantage of this material system is its controllable thermoelastic behaviour wins a lamination tailoring technique. In spacecraft applications, in particular, a small coefficient of thermal expansion (CTE) is one of the most desirable properties of the structural components. A typical example is a tubular member of three-dimensional truss as fundamental parts of a huge space station. A large ladder-like framework made of aluminium alloy will deform or vibrate seriously by a transient temperature gradient in the space environment. Such vibration degrades a level of microgravity, which is one of the fundamental missions of the space station.

It is widely understood that an employment of graphite–epoxy composites provides more thermally stable structures than metallic materials. However, the CTE is not small enough for general graphite–epoxy laminates. Hence, a lamination tailoring technique based on a graphical procedure has recently been investigated in order to reduce the CTE of this material system. It is discovered that a tailored laminate should exhibit a very low CTE in a principal direction under a wide range of temperatures in the space environment. The present paper demonstrates a basic theory and some results of early experimental verification. Serious anisotropy in thermal expansion properties [1] peculiar to graphite–epoxy composites makes this idea possible.

## 2. Background and theoretical description

### 2.1. Background

Early work [2, 3] indicated that certain angle-ply graphite–epoxy laminates should have null CTE in one direction at one specific temperature. Theoretical and experimental results [2] are quoted here as Fig. 1 and a quite similar diagram is given in [3]. The expected angle, $\theta_0$, for zero CTE is approximately 42° in both papers [2, 3]. Such characteristics are mainly caused by a small negative CTE in the fibre direction and the highly anisotropic elastic properties of unidirectional graphite–epoxy composites. In practice, however, it is very difficult to obtain a null-expansion angle-ply laminate because most polymeric matrices show serious temperature dependency in their stiffness and CTE. An improvement of this fundamental defect is the goal of the present work.

This goal is achieved by an easy-to-use graphical procedure for the specification of the CTE in a wide range of temperatures. The concept of the lamination parameters developed by one of the authors (HF) [4] is an essential basis for the present theory. The concept of lamination parameters stems from a manipulation of stiffness invariants slightly different from the Tsai's [5] established description. The present formulation is based on $\cos 2\theta$, $\sin 2\theta$ and their square, whereas the Tsai's formulation uses $\cos 2\theta$, $\sin 2\theta$, $\cos 4\theta$ and $\sin 4\theta$ and so on. The utilization of the square terms is a key-point for an easier graphical presentation and a visual optimization procedure.

### 2.2. Thermoelastic invariants

Another key concept of the present work is an introduction of thermoelastic invariants consistent with the above-mentioned formulation in order to incorporate the thermal expansion behaviour into the classical laminate theory. Hence, the present definition of the invariants is different from that of Miller [6] who was, to the authors' knowledge, the first to treat this problem. The thermoelastic invariants denoted by

0022–2461/89 $03.00 + .12 

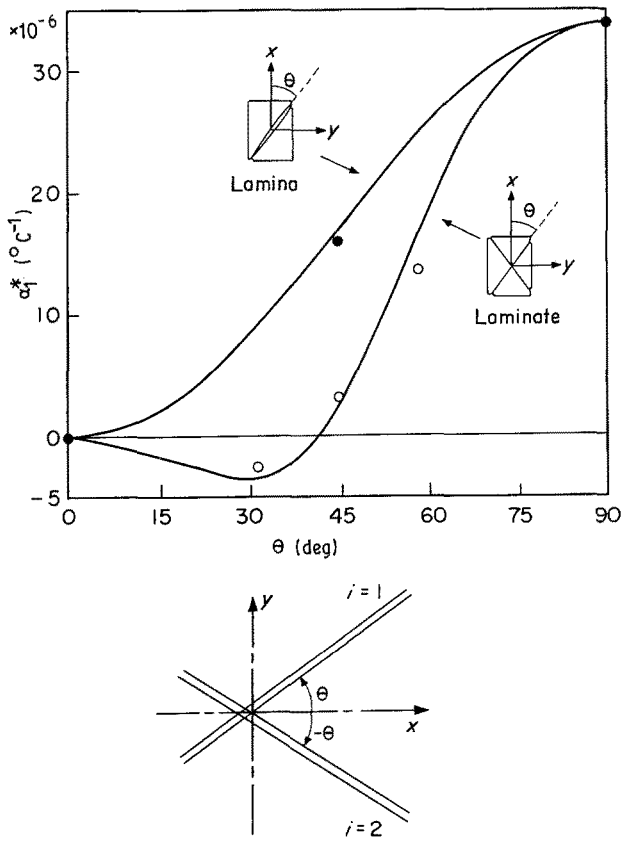


*Figure 1* Effect of an off-axis angle, $\theta$, upon the CTE's of unidirectional and angle-ply graphite–epoxy materials reported in [2].

$q_1^*$ and $q_2^*$ can be defined as follows

$$q_1^* = Q_{11}\alpha_L + Q_{12}(\alpha_T + \alpha_L) + Q_{22}\alpha_T$$
$$q_2^* = Q_{11}\alpha_L + Q_{12}(\alpha_T - \alpha_L) - Q_{22}\alpha_T \quad (1)$$

where $Q_{ij}$ are on-axis components of two-dimensional reduced stiffness of unidirectional composites [7], and $\alpha_L$ and $\alpha_T$ are the longitudinal and transverse CTE's of UD materials. With the introduction of these quantities, we can now describe a transformation formula of a thermoelastic vector of the $m$th lamina denoted by $q_i^{(m)}(\theta)$ under an off-axis angle, $\theta$, as follows

$$q_i^{(m)}(\theta) = \frac{1}{2}\begin{Bmatrix} q_1^* + q_2^* \cos 2\theta \\ q_1^* - q_2^* \cos 2\theta \\ q_2^* \sin 2\theta \end{Bmatrix} \quad (2)$$

where $q_i^{(m)}(\theta) = Q_{ij}^{(m)}(\theta)\alpha_j^{(m)}(\theta)$, and where $\alpha_j^{(m)}(\theta)$ is a vector description of the CTE of the $m$th lamina. A constitutive equation of a laminate with a small temperature increment $\Delta T$ can be written in the following form [8]

$$\begin{Bmatrix} N \\ M \end{Bmatrix} = \begin{bmatrix} A & B \\ B & D \end{bmatrix}\begin{Bmatrix} \varepsilon^0 \\ \chi \end{Bmatrix} - \Delta T \begin{Bmatrix} \tilde{A} \\ \tilde{B} \end{Bmatrix} \quad (3)$$

where $(\tilde{A}_i, \tilde{B}_i) = \Sigma_{m=1}^{N} \int_{h_{m-1}}^{h_m} (1, z) q_i^{(m)} \mathrm{d}z$ $(i = 1, 2, 6)$ and where $q_i^{(m)} = Q_{ij}^{(m)}\alpha_j^{(m)}$ or in the inverted form

$$\begin{Bmatrix} \varepsilon^0 \\ \chi \end{Bmatrix} = \begin{bmatrix} a^* & b^* \\ b^* & d^* \end{bmatrix}\begin{Bmatrix} N \\ M \end{Bmatrix} + \Delta T \begin{Bmatrix} \tilde{a}^* \\ \tilde{b}^* \end{Bmatrix} \quad (4)$$

where

$$\begin{Bmatrix} \tilde{a}^* \\ \tilde{b}^* \end{Bmatrix} = \begin{bmatrix} a^* & b^* \\ b^* & d^* \end{bmatrix}\begin{Bmatrix} \tilde{A} \\ \tilde{B} \end{Bmatrix} \quad (5)$$

It should be noted that $\tilde{a}_i^*$ in Equation 4 denotes an in-plane CTE of the laminate. By substituting Equation 2 into Equation 5 and considering that $q_1^*$ and $q_2^*$ are invariants with respect to $\theta$, we have the following results of integration for $\tilde{A}_i$

$$\tilde{A}_i = \frac{h}{2}\begin{Bmatrix} q_1^* + q_2^* \int_0^1 \cos 2\theta \, \mathrm{d}u \\ q_1^* - q_2^* \int_0^1 \cos 2\theta \, \mathrm{d}u \\ q_2^* \int_0^1 \sin 2\theta \, \mathrm{d}u \end{Bmatrix} \quad (6)$$

## 2.3. Lamination parameters

If we define the above integrations of circular functions of off-axis angles as the parameters related to the lamination construction, we can systematically treat some problems of composite laminates. Hence, these quantities will henceforth be referred to as lamination parameters. As stated earlier, this concept was proposed and used for some optimization problems by Fukunaga [4]. All the definitions of $\xi_1$ to $\xi_4$ are described below.

$$\xi_1 = \int_0^1 \cos 2\theta \, \mathrm{d}u, \quad \xi_2 = \int_0^1 \cos^2 2\theta \, \mathrm{d}u$$
$$\xi_3 = \int_0^1 \sin 2\theta \, \mathrm{d}u, \quad \xi_4 = \int_0^1 \sin 2\theta \cos 2\theta \, \mathrm{d}u \quad (7)$$

In the case of a practical laminate, the total amounts of the $+\theta$ and $-\theta$ layers are the same, and the stacking sequence is symmetric with respect to the geometrical midplane. The laminates with the former condition are referred to as balanced laminates, and $\xi_3$ and $\xi_4$ vanish for these laminates. Thus, the design of the laminate construction in the two-dimensional space of $\xi_1$ and $\xi_2$ is essential.

The ranges of integrands of $\xi_1$ and $\xi_2$ are as follows

$$-1 \leqslant \cos 2\theta \leqslant 1, \quad 0 \leqslant \cos^2 2\theta \leqslant 1 \quad (8)$$

It is understood that a region above a parabola of $\xi_2 = \xi_1^2$ is feasible. Fig. 2 depicts the resulting shape of the feasible region. Note that the parabola corresponds to angle-ply laminates consisting of $\pm\theta$ layers, and that the upper straight line corresponds to cross-ply laminates. The right and left apexes indicate 0° and 90° UD materials, respectively. The bold lines denote iso-stiffness conditions in one principal direction explained later in Equation 12.

## 2.4. Formulation of an explicit description of a CTE

We can take an advantage of the idea of the lamination parameters in the present problem. The condition of balanced and symmetrical laminates renders the formulation much simpler. Two lamination parameters, $\xi_3$ and $\xi_4$, vanish as do $\tilde{B}_i$ and $B_{ij}$ in Equations 3 and 4. Hence, Equation 4 is reduced to

$$\tilde{a}_i^* = a_{ij}^* \tilde{A}_j \quad (9)$$

where $a_{ij}^* = A_{ij}^{-1}$. Then, we have an explicit expression of $\tilde{A}_i$ in this equation by substituting the lamination parameters into Equation 6

$$\tilde{A}_i = \tfrac{1}{2}h(q_1^* + q_2^*\xi_1, q_1^* - q_2^*\xi_1, q_2^*\xi_3) \quad (10)$$

The next step of the analysis is an explicit description

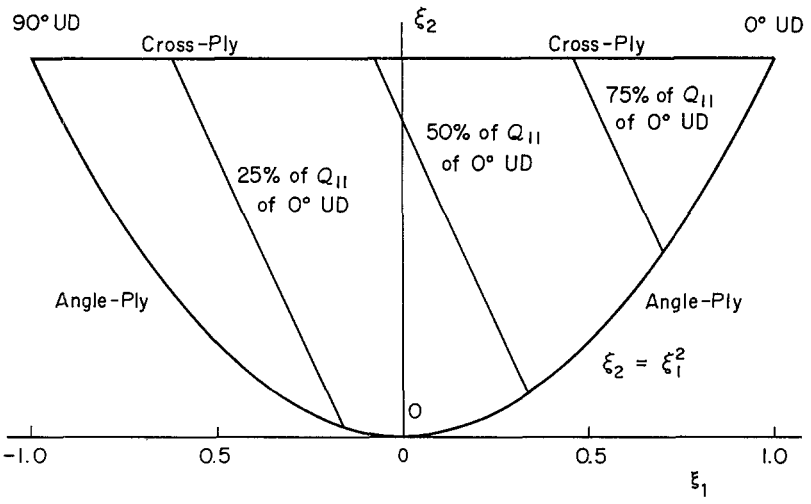


*Figure 2* Feasible region of the lamination parameters, $\xi_1$ and $\xi_2$.

of $a_{ij}^*$ in Equation 9 in the consistent manner with the above formulation. In-plane stiffness invariants can be written as follows [9]

$$\begin{aligned} U_1 &= [Q_{11} + 2(Q_{12} + 2Q_{66}) + Q_{22}]/4 \\ U_2 &= (Q_{11} - Q_{22})/2 \\ U_3 &= [Q_{11} - 2(Q_{12} + 2Q_{66}) + Q_{22}]/4 \\ U_4 &= \{Q_{11} + 2(Q_{12} - 2Q_{66}) + Q_{22}\}/4 \\ U_5 &= (Q_{11} + Q_{22} - 2Q_{12})/4 \end{aligned} \quad (11)$$

By using these invariants, we have the following expressions of the components of the in-plane stiffness matrix of a balanced laminate, $A_{ij}$, with $\xi_1$ and $\xi_2$

$$\begin{aligned} A_{11} &= h(U_1 + U_2\xi_1 + U_3\xi_2) \\ A_{12} &= h(U_4 - U_3\xi_2) \\ A_{22} &= h(U_1 - U_2\xi_1 + U_3\xi_2) \\ A_{66} &= h(U_5 - U_3\xi_2) \end{aligned} \quad (12)$$

The first equation of Equation 12 gives the iso-stiffness lines of Fig. 2. Equations 9 and 10 can be rewritten for an explicit expression of a CTE in the 1 direction, as

$$\tilde{a}_1^* = \frac{[A_{22}(q_1^* + q_2^*\xi_1) - A_{12}(q_1^* - q_2^*\xi_1)]h}{[2(A_{11}A_{22} - A_{12}^2)]} \quad (13)$$

By substituting Equation 12 into Equation 13, we have

$$\tilde{a}_1^* = \frac{(U_1 - U_2\xi_1 + U_3\xi_2)(q_1^* + q_2^*\xi_1) - (U_4 - U_3\xi_2)(q_1^* - q_2^*\xi_1)}{2[(U_1 + U_2\xi_1 + U_3\xi_2)(U_1 - U_2\xi_1 + U_3\xi_2) - (U_4 - U_3\xi_2)^2]} \quad (14)$$

This explicit description of the CTE of a balanced symmetric laminate with thermoelastic invariants, elastic invariants and lamination parameters is a milestone of the present technique.

### 2.5. Condition for specified value of CTE

The goal of the present paper is to control a CTE at a specified value, $\alpha_s$. This goal is simply reached by substituting $\alpha_s$ to the left-hand side of Equation 14. After some manipulations, equation 14 can be rewritten into the following quadratic function of $\xi_1$

$$\xi_2 = \frac{U_2(q_2^* - 2\alpha_s U_2)\xi_1^2 - [(U_1 + U_4)q_2^* - U_2 q_1^*]\xi_1}{2U_3[q_1^* - 2\alpha_s(U_1 + U_4)]} + (U_4 - U_1)/2U_3 \quad (15)$$

The most practically important target is a null CTE laminate. By substituting $\alpha_s = 0$ into Equation 15, we have the following form

$$\xi_2 = \{U_2(q_2^*/q_1^*)\xi_1^2 - \xi_1[(U_1 + U_4)q_2^* - U_2 q_1^*]/q_1^* + U_4 - U_1\}/2U_3 \quad (16)$$

It should be noted that these equations are graphically expressed as segments of parabolae in the feasible region of the lamination parameters. Thus, we can obtain a laminate with a controlled CTE in one direction by using certain combinations of $\xi_1$ and $\xi_2$ on such a parabola. An application of this procedure with temperature dependent material properties is the point of the next section.

## 3. Numerical results based on actual material data

### 3.1. Basic material properties

Temperature dependent material properties of the constituent unidirectional graphite–epoxy composites have a serious influence upon the present CTE-control problem. The most dominant material property on the tailored laminate is an axial CTE of the UD lamina. The experimental results for a wide range of temperatures given by Yates *et al.* [11] are employed for a high strength graphite–epoxy composite. Fig. 3 is reproduced from reference [11] and some experimental data obtained by one of the authors (TI)[1] are additionally indicated by full squares. It can be observed that there exists serious scatter in $\alpha_L$ along with a temperature change. Three straight lines represent the highest, middle and the lowest scatter of the data, respectively.

Among other factors governing the CTE of polymeric composites, moisture has a certain effect upon $\alpha_L$ and $\alpha_T$ as pointed out by Ishikawa *et al.* [1]. Hygroscopically stabilized CTE values, therefore, should be employed here. Some precautions are required at experimental verification in order to avoid the hygroscopic effect.

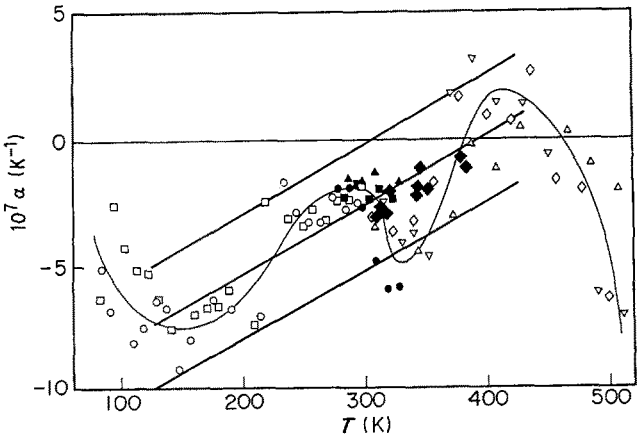


*Figure 3* Detailed experimental results of longitudinal CTE's of the UD lamina quoted from references [1] (◆) and [11].

### 3.2. Intersection of zero-CTE condition at various temperatures

On the basis of the temperature dependent data of the six properties, a calculation of Equation 16 is conducted for some levels of temperature. Three temperatures, 123, 300 and 423 K, are chosen and the values of the six properties are given in Table I. Three values of $\alpha_L$ are assigned correspondingly to the scatter indicated in Fig. 3.

Fig. 4 depicts the results based on the middle line. Note that only the right-hand half of the feasible region of the lamination parameters explained in Fig. 2 is indicated for simplicity. It is clearly shown that segments of the parabola obtained by Equation 16 cross each other almost at one point, $(\xi_1, \xi_2) = (0.337, 0.406)$. Although the results at other temperature levels are not indicated here, they fall between the plotted curves and meet almost at one point in the $\xi_1$–$\xi_2$ plane. This fact demonstrates that the laminate with an intersectional combination of $\xi_1$ and $\xi_2$ will exhibit an approximately null CTE in one direction in the wide range of temperatures.

As stated earlier, an angle-ply laminate with $\theta_0 = 42°$ does not expand only around room temperature. This property is easily understood through Fig. 4. The intersection point of the parabola of $\xi_2 = \xi_1^2$ and the CTE free curve at 300 K corresponds to the above-mentioned angle-ply material. At higher or lower temperatures, this material system will expand to some extent. It is also important that the intersectional set of $\xi_1$ and $\xi_2$ in Fig. 4 provides much higher in-plane stiffness than the angle-ply laminate with $\theta_0 = 42°$.

It should be noted that a similar conclusion is derived based on the longitudinal CTE data expressed by the highest line. Moreover, the fibre volume fraction denoted by $V_f$ also seriously affects the present technique because the six basic material properties are susceptible to $V_f$.

### 3.2. A laminate construction for the specified lamination parameters

A determination of a laminate construction for the specified set of the lamination parameters is an inverse problem of the procedures of Equation 7. Although a general consideration like the recent work of one of the authors (HF) [12] is possible, it seems to be outside the content of the present paper. If the construction is confined to symmetric laminates of $(0°, \pm\theta)$, this inverse problem is easily solved. Let us denote ratios of 0° and $\pm\theta$ layers to a total thickness by $\zeta$ and $\eta$, respectively. Thus, we have

$$\zeta + \eta = 1 \tag{17}$$

The problem is interpreted as the determination of $\zeta$ or $\eta$, and $\theta$ to obtain a specified set of $(\xi_1, \xi_2)$. From

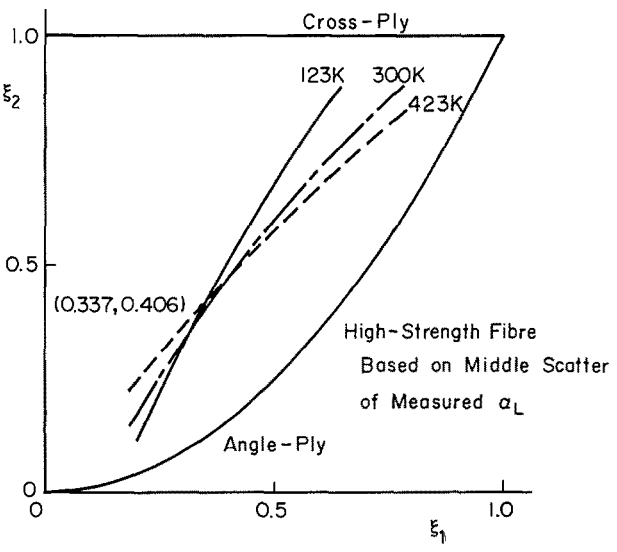


*Figure 4* CTE free curves in the feasible region of the lamination parameters based on the middle scatter of the data of $\alpha_L$.

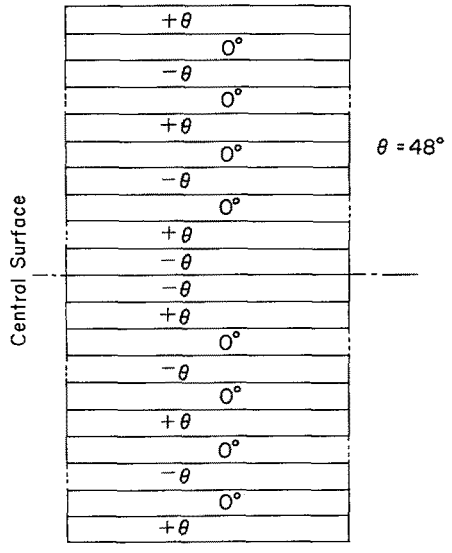


*Figure 5* An example of a symmetric laminate construction for a set of lamination parameters (0.337, 0.406).

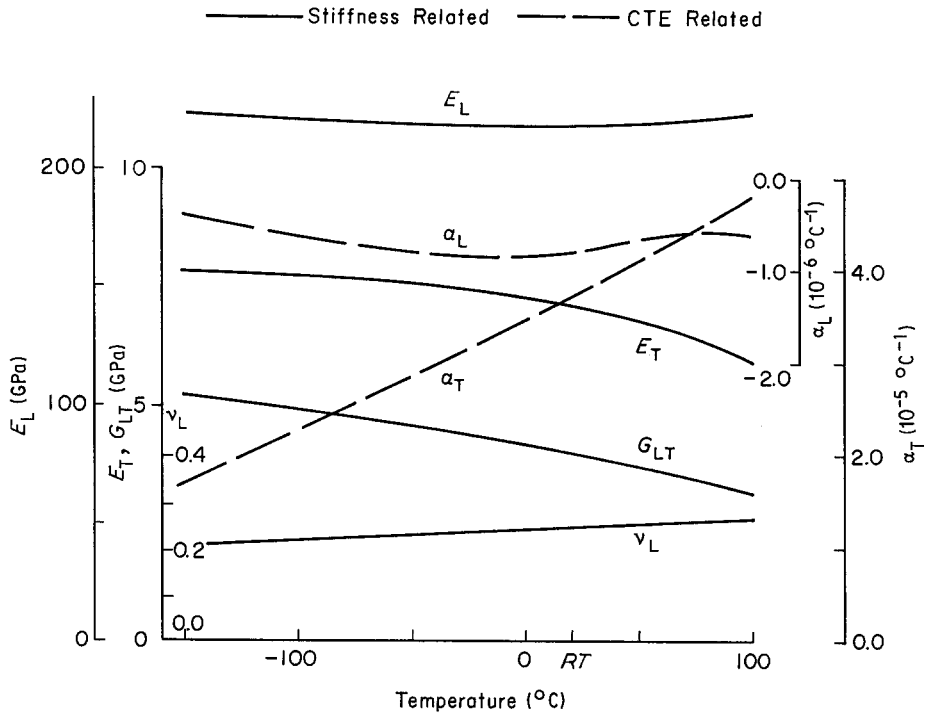


*Figure 6* Temperature dependent material data of high-modulus graphite–epoxy UD system.

a consideration of Equation 7, we have the following equations

$$\zeta + \eta \cos 2\theta = \xi_1$$
$$\zeta + \eta \cos^2 2\theta = \xi_2 \quad (18)$$

The simultaneous Equations 17 and 18 are manipulated into

$$\cos 2\theta = (\xi_1 - \xi_2)/(1 - \xi_1)$$
$$\eta = (1 - \xi_1)/(1 - \cos 2\theta) \quad (19)$$

The first equation of Equation 19 gives $\theta$ and then $\eta$ or $\zeta$ is obtained. From a practical point of view, the values of $\eta$ or $\zeta$ are not arbitrary because the number of thicknesses of commercially supplied prepreg is limited. Hence, some adjustments of Equation 19 are always required and thick laminates are advantageous for precise tailoring.

An example of the laminate construction which gives a set of $(\xi_1, \xi_2) = (0.337, 0.406)$ corresponding to the intersection in Fig. 4 is shown in Fig. 5. It should be noted that the value of $\eta$ or $\zeta$ determines the quantity of the layers but does not provide any information about lamination sequence. Therefore, the sequence in Fig. 5 is determined based on some practical experience within the restriction of symmetry. As stated earlier, the lamination angle, $\theta$, is dependent upon the fibre volume fraction.

### 3.3. Results for high modulus graphite–epoxy

Fig. 4 only gives the results for high strength graphite–epoxy composites. In common spacecraft structures, high modulus graphite–epoxy composites are more widely employed. Hence, it is worthwhile examining the solution of the present technique for this material system. The basic properties of the unidirectional high-modulus graphite–epoxy composites are shown in Fig. 6. Behaviour of $\alpha_L$ distinct from that of the high-strength graphite–epoxy composite can be clearly seen. Fig. 7 depicts the segments of the null CTE

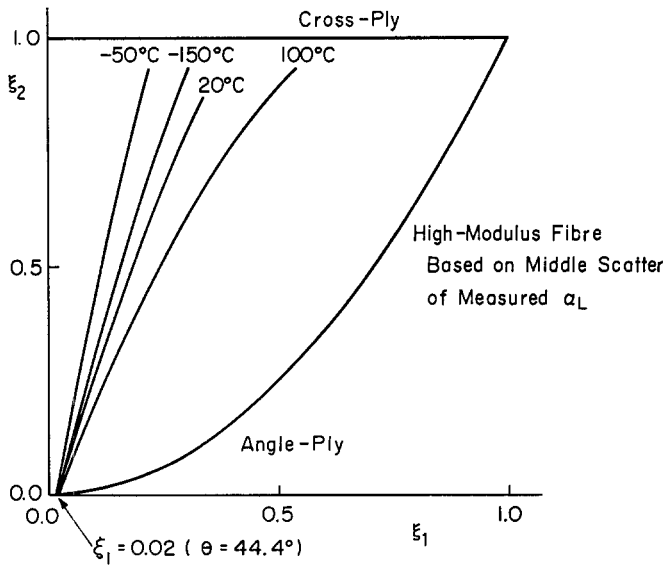


*Figure 7* CTE free curves in the feasible region of the lamination parameters for high-modulus graphite–epoxy material.

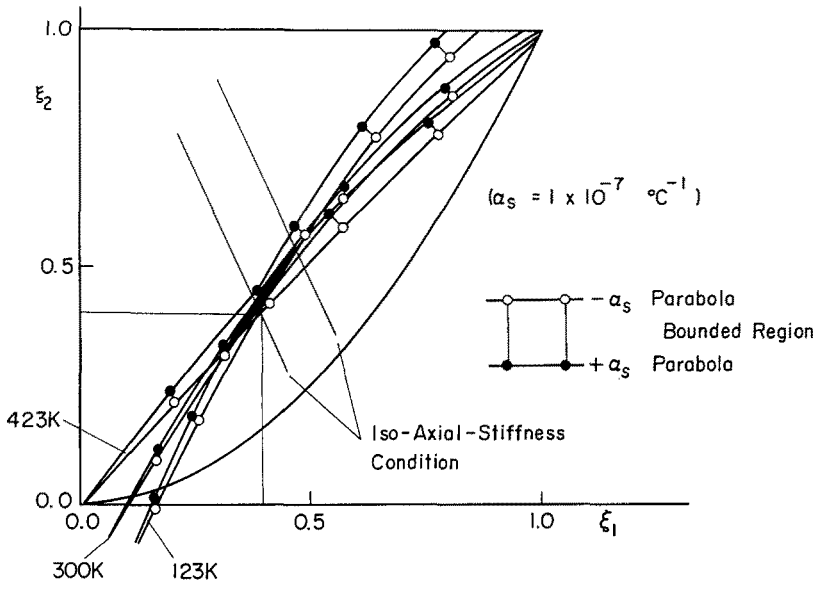


*Figure 8* A shape of the feasible region where a CTE value within $\pm 1 \times 10^{-7}\,°C^{-1}$ is permitted.

parabolae at four temperatures. They cross each other almost on the edge of the feasible region which corresponds to an angle-ply laminate with an angle of 44.4°. This result implies that the present technique does not provide a practical material system for the high-modulus graphite–epoxy composites because such an angle-ply laminate has quite low axial stiffness coefficient.

### 3.4. Allowance for very small CTE

The present technique can be easily expanded to the case where a very small CTE is allowed in one direction. A parabola for the specified CTE, $\alpha_s$, is determined from Equation 15 and the six material properties at a level of temperature. If we set an allowance of a CTE within $\pm\alpha_s$, we have a feasible region of lamination parameters bounded by two parabolae. By repeating this procedure for many temperatures, we can obtain a meeting of the regions which the CTE is limited to a small value within $\alpha_s$. The result based on $\alpha_s = 1 \times 10^{-7}\,°C^{-1}$ and the material properties for the middle scatter in Table I is shown in Fig. 8. A central lenticular region represents the solution and inclined lines denote iso-axial-stiffness conditions. Thus, we can find the set of the lamination parameters of the highest axial stiffness within the allowance of a small CTE.

## 4. Results of experimental verification in a higher temperature range

Some preliminary measurements of the CTE in one principal direction are conducted for the tailored laminate. Due to the inhomogeneity and the finite width of the specimens, a certain influence of the edge effect may be inevitable. Hence, the larger ratio of the width to the thickness is strongly recommended, or thin tubes may be ideal. In the present experiments, plate specimens of 25 mm in width and 1 mm in thickness are used. A laminate construction indicated in Fig. 5 is adopted here. The fibre angle $\theta$ is determined to 46.4° based upon an average fibre volume fraction of the specimens of 60%. The length of specimens is 50 mm corresponding to a conventional thermal extensometer using standard quartz pieces.

Seven specimens are tested and the detailed results of pieces 1 and 7 for a temperature increment of 5° C

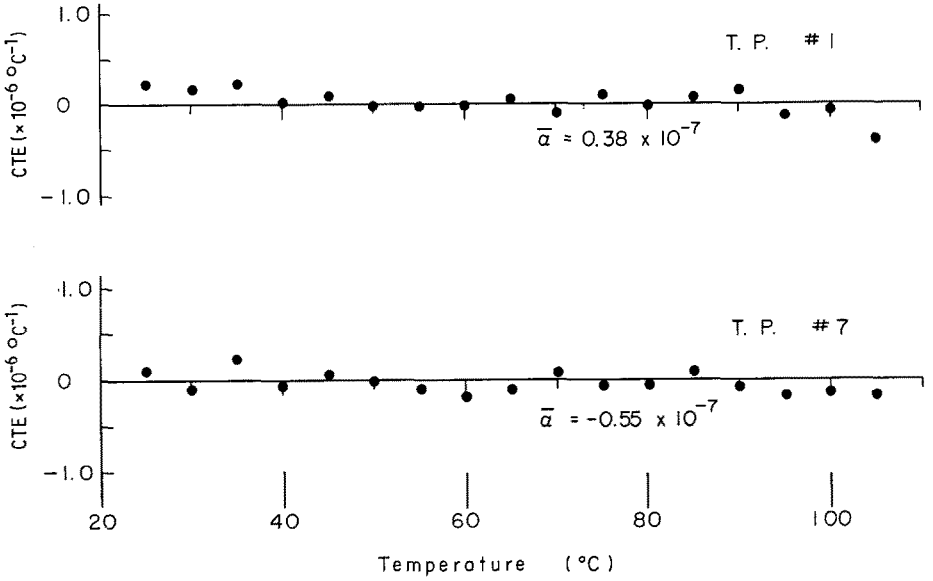


*Figure 9* Examples of near-zero CTE data measured by a thermal extensometer.

TABLE I Six independent material properties of unidirectional graphite–epoxy lamina at 123, 300 and 423 K

| | 123 K | 300 K | 423 K |
|---|---|---|---|
| $E_L$ (GPa) | 137 | 135 | 133 |
| $E_T$ (GPa) | 20 | 11 | 2 |
| $G_{LT}$ (GPa) | 10 | 5.5 | 0.5 |
| $\nu_L$ | 0.29 | 0.3 | 0.35 |
| $\alpha_T$ ($°C^{-1}$) | 1.9 | 3.2 | 4.1 |
| $\alpha_L$ ($°C^{-1}$) | −0.5 | −0.01 | 0.33 |
| Highest | ( | $\times 10^{-6}$ | ) |
| $\alpha_L$ ($°C^{-1}$) | −0.75 | −0.26 | 0.08 |
| Middle | ( | $\times 10^{-6}$ | ) |
| $\alpha_L$ ($°C^{-1}$) | −1.01 | −0.52 | −0.18 |
| Lowest | ( | $\times 10^{-6}$ | ) |

are shown in Fig. 9. The data fall around the zero CTE although slight deviations are found. Simple averages of $\alpha$ are values of minus eighth order of 10 as indicated. Scatters of the results among seven specimens are trivial. Such results demonstrate that an initial attempt of the present technique is fairly successful at least in a range of temperature higher than room temperature. Verifications in the lower range of temperature will be conducted in the quite near future.

## 5. Concluding remarks

A lamination tailoring technique for the control of a CTE in one principal direction is proposed. This technique consists of two theoretical concepts; the thermoelastic invariants and the lamination parameters. The CTE free condition yields to a parabola in the feasible region of the lamination parameters. The segments of the parabola calculated for a wide range of temperature intersect almost at a point. A laminate with the construction corresponding to this point provides an approximately zero CTE in one direction in this temperature range. This technique is easily expanded to the optimization procedure under the restriction of a small allowance of the CTE. Experimental verifications demonstrate that the present scheme is practically possible. If graphite–epoxy tubes tailored so as to suppress the CTE are adopted for the structure of the space station, its thermal deformation will vanish almost completely.

## Acknowledgement

The authors wish to express their sincere gratitude to Mr K. Kawakami of Mitsubishi Electric Company Ltd. for his great assistance in the experiments.

## References

1. T. ISHIKAWA, K. KOYAMA and S. KOBAYASHI, *J. Compos. Mater.* **12** (1978) 153–168.
2. K. F. ROGERS, L. N. PHILLIPS, D. M. KINGSTON-LEE, B. YATES, M. J. OVERY, J. P. SARGENT and B. A. McCALLA, *J. Mater. Sci.* **12** (1977) 718–733.
3. M. UEMURA, Y. YAMAGUCHI and H. IYAMA, *J. Jpn Soc. Space Aeronautical Sci.* **26** (1978) 471–479 (in Japanese).
4. H. FUKUNAGA, *ibid.* **28** (1981) 482–489 (in Japanese).
5. S. W. TSAI and H. T. HAHN, "Introduction to Composite Materials" (Technomic, Westport, CT., 1980).
6. A. K. MILLER, *Fibre Sci. Technol.* **13** (1980) 397–409.
7. R. M. JONES, "Mechanics of Composite Materials" (McGraw-Hill, New York, 1975).
8. T. ISHIKAWA and T. W. CHOU, *J. Compos. Mater.* **17** (1983) 92–104.
9. H. FUKUNAGA, "Stiffness and/or Strength Optimization of Laminated Composites", Proceedings of 3rd Japan–US Conference of Composite Materials, Tokyo, 1986, (Japan Society Compos. Mater.) pp. 655–662.
10. T. ISHIKAWA, T. TAKI and S. KOBAYASHI, *J. Jpn Soc. Space Aeronautical Sci.* **27** (1979) 370–378 (in Japanese).
11. B. YATES, M. J. OVERY, J. P. SARGENT, B. A. McCALLA, D. M. KINGSTON-LEE, L. N. PHILLIPS and K. F. ROGERS, *J. Mater Sci.* **13** (1978) 433–440.
12. H. FUKUNAGA, *J. Jpn Soc. Compos. Mater.* **13** (1987) 107–115 (in Japanese).

*Received 8 February*
*and accepted 13 June 1988*